ACS APPLIED MATERIALS & INTERFACES

RESEARCH ARTICLE

www.acsami.org

Influence of WC-Co Substrate Pretreatment on Diamond Film Deposition by Laser-Assisted Combustion Synthesis

Amélie Veillère,[†,‡] Thomas Guillemet,[†,‡] Zhi Qiang Xie,[†] Craig A. Zuhlke,[†] Dennis R. Alexander,[†] Jean-François Silvain,[‡] Jean-Marc Heintz,[‡] Namas Chandra,[§] and Yong Feng Lu*[,†]

[†]Department of Electrical Engineering, University of Nebraska, Lincoln, Nebraska 68588-0511, United States

[‡]CNRS, Université de Bordeaux, ICMCB, 87 Avenue du Docteur Albert Schweitzer, F-33608 Pessac, France

[§]Department of Mechanical Engineering, University of Nebraska, Lincoln, Nebraska 68588-0642, United States

ABSTRACT: The quality of diamond films deposited on cemented tungsten carbide substrates (WC-Co) is limited by the presence of the cobalt binder. The cobalt in the WC-Co substrates enhances the formation of nondiamond carbon on the substrate surface, resulting in a poor film adhesion and a low diamond quality. In this study, we investigated pretreatments of WC-Co substrates in three different approaches, namely, chemical etching, laser etching, and laser etching followed by acid treatment. The laser produces a periodic surface pattern, thus increasing the roughness and releasing the stress at the interfaces between the substrate and the grown diamond film. Effects of these pretreatments have been analyzed in terms of microstructure and cobalt content. Raman spectroscopy was conducted to characterize both the diamond quality and compressive residual stress in the films.

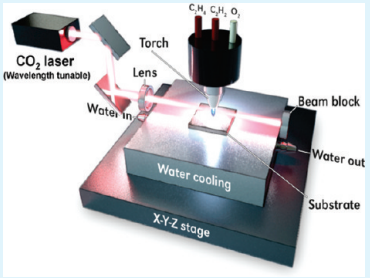

KEYWORDS: diamond, substrate pretreatment, chemical and laser etchings, cobalt diffusion, residual stress, Raman spectroscopy

1. INTRODUCTION

Diamond exhibits extreme hardness, high wear resistance, and high thermal conductivity. It is therefore an ideal coating material for cutting tools. In the past 60 years, many studies have been conducted for diamond deposition and several techniques have been developed to improve the diamond growth.[1−3] The most popular method is low-pressure chemical vapor deposition (CVD). Since the first report of diamond combustion synthesis in 1988 by Hirose and Kondo,[3] this method has been demonstrated as one of the most promising approaches for growing diamond due to its flexibility (open-air system, no substrate size limitation), low-cost, and high growth rate.[4] Recently, a modified combustion-CVD technique has been developed with significant improvement on diamond quality and growth rate.[5−7] This technique, used in this study, couples the conventional combustion flame method with a high-power wavelength-tunable CO_2 laser to excite the ethylene precursor molecules for increased growth rate.

Although remarkable advancements have been made in diamond deposition, diamond coating on cemented tungsten carbide (WC-Co) substrates remains difficult. The main problem is the lack of strong adhesion between the substrates and the diamond films because of considerable differences in their thermo-mechanical properties (thermal expansion and elastic modulus). Various techniques are currently applied to decrease the residual stress and prevent delamination, such as chemical and physical etching and thermal treatment.[8−10] These techniques increase the surface roughness of the substrates and provide more anchoring sites for diamond growth and hence higher adhesion strength.

One issue with WC-Co substrates is the presence of cobalt as binder in the cemented tungsten carbide, which can catalyze the formation of nondiamond carbon forms (sp^2 carbon).[11,12] These nondiamond carbon forms have a detrimental effect on the formation of diamond (sp^3 carbon) and degrade adhesion between the coatings and the substrates. To remove the cobalt and/or decrease its migration to the surface, many pretreatments have been investigated: chemical etching (HNO_3, Murakami's reagent, Caro's acid, ...),[10−16] high-energy ion irradiation,[8,9,17] deposition of diffusion barrier layers (nitride or carbide compounds).[10,15,16]

The purpose of this work is to investigate the influence of various WC-Co substrate pretreatments on the quality and adhesion of the diamond films, including: chemical etching with Murakami's reagent followed by an acid attack, laser etching, and laser etching coupled with the acid attack. The surface morphology, cobalt content, quality and residual stress of diamond films have been characterized for each substrate pretreatment using Scanning Electron Microscopy (SEM), Atomic Force Microscopy (AFM), Electron Probe MicroAnalysis (EPMA), and Raman spectroscopy.

2. EXPERIMENTAL DETAILS

2.1. Substrate Pretreatment. Tungsten carbide (WC-Co) substrates from Basic Carbide Corporation, with 6 wt % of cobalt and a dimension of 12.7 × 12.7 × 1.6 mm^3 were used. The substrates were submitted to a chemical etching or laser etching to study the influence of each pretreatment on the diamond film quality and adhesion by comparison with an untreated substrate (named P0). Before each pretreatment (summarized in Table 1), the substrates were ultrasonically cleaned in acetone for 30 min.

Received: December 26, 2010
Accepted: April 4, 2011
Published: April 04, 2011

Table 1. WC-Co Substrates Pretreatment Designations and Specifications

pretreatment name	pretreatment conditions
P0	original substrate
P1	6 min in Murakami reagent and 30 s in (HNO_3 + H_2O_2) solution
P2	laser irradiation
P3	laser irradiation and 30 s in (HNO_3 + H_2O_2) solution

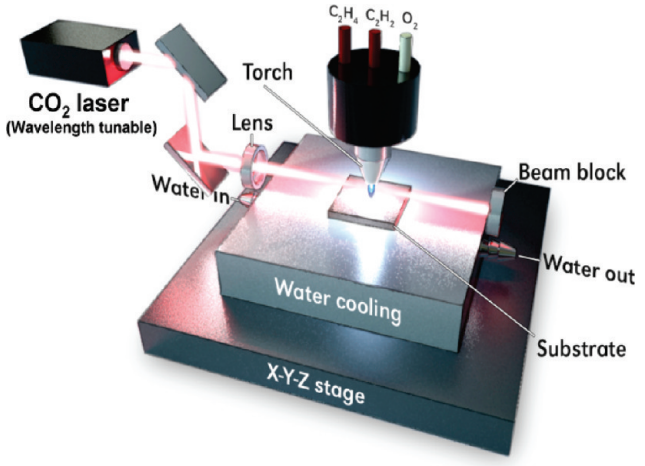

Figure 1. Schematic setup for the laser-assisted combustion CVD of diamond films.

The first pretreatment (named P1) is a conventional chemical etching using Murakami's reagent followed by dissolution of the inserted cobalt by an acid attack. The substrate was etched by the Murakami's solution (5 g $K_3[Fe(CN)_6]$ + 5 g KOH + 50 mL H_2O) for 6 min at room temperature and rinsed in deionized water. This first step allows preferential etching of the WC substrate and leaves the cobalt particles unaffected on the surface. The cobalt particles are then removed using an acid treatment (a mixture of 5.1 mL HNO_3 and 9 mL H_2O_2) for 30 s followed by rinsing in deionized water.

The second pretreatment (named P2) is a physical etching. The surface roughness of the substrate was modified using a Ti sapphire femtosecond (fs) laser in ambient air conditions. One advantage of using fs lasers over longer pulsed lasers is the minimized heat affected zone (HAZ).[18] Indeed, the shorter the laser pulses are, the smaller the resulting HAZs will be in the material. With femtosecond lasers, the surface of a material can be altered without affecting the bulk of the sample. The laser wavelength is centered at around 800 nm with a maximum energy of 1 mJ with a 50 fs pulse width at a 1 kHz repetition rate. A planoconvex cylindrical lens made of fused silica with a focal length of 150 mm was used to focus the femtosecond laser into a line onto the sample surfaces. On the basis of the single shot ablation of the surface, the focused line was 22 μm × 3.22 mm. The sample was rastered perpendicular to the long axis of the line focus. The laser beam has a Gaussian profile. The sample was processed in the region before the laser focus. With a line width of 22 μm and a repetition rate of 1 kHz each spot was illuminated by the laser 11 times in each rastering pass. The step size between rastering passes was 300 μm. For a line width of 3.22 mm, each location was illuminated from consecutive rastering passes about 10 times. A set of Melles Griot Nanomotion II translation stages, controlled by a computer, were used to translate the samples. The laser-induced periodic surface structures (LIPSS) were produced on the substrate surfaces using a laser power of 780 mW and a motion speed of 2 mm/s. The power reached the substrate surface was 625 mW, resulting in a fluence of 882 mJ/cm^2. The polarization of the incident laser was perpendicular to the direction of the LIPSS lines.

The last pretreatment (named P3) is a combination of laser and chemical etchings. In this case a laser irradiation was performed under the same conditions as P2, followed by an acid attack with a mixed solution of HNO_3 and H_2O_2 (5.1 and 9 mL, respectively) for 30 s.

2.2. Diamond Deposition. Diamond films were deposited using a laser-assisted combustion flame system in open air as shown in Figure 1. The experimental setup has been described in details elsewhere.[5−7] In this system, a wavelength-tunable CO_2 laser (XL1000, PRC Laser Corporation) was associated to a combustion flame system. The gas precursor is a mixture of acetylene (C_2H_2, 99.999%), ethylene (C_2H_4, 99.6%), and oxygen (O_2, 99.996%) with a volume ratio of 1:1:2, respectively. The laser power was set at 800 W and the wavelength at 10.532 μm to match the vibrational mode of ethylene molecules and increase the diamond growth.[5,6,19] The substrate was placed under the torch using a motorized $X-Y-Z$ stage. The substrate temperature was measured by an infrared pyrometer (OS3752, Omega Engineering, Inc.) and maintained around 780 °C during diamond deposition using a water-cooling system. The diamond films were deposited for 15 and 60 min to analyze, for the first deposition time, the first step of nucleation and, for the second one, the residual stress in the films.

2.3. Microstructural and Chemical Analyses. The morphology of the diamond films was analyzed using a field-emission Scanning Electron Microscope (FESEM, Hitachi S4700). Atomic Force Microscopy (AFM, Digital instrument Nanoscope IIIa dimension 3100) was carried out in the tapping mode on the substrate after each pretreatment so as to investigate their impact on the surface topography. This analysis was performed on a 4 μm × 4 μm area on each sample. The cobalt concentrations on the WC-Co substrate, before diamond deposition, were measured using electron probe microanalyses (EPMA, CAMECA SX 100) equipped with wavelength dispersive spectrometry (WDS), with an accelerating voltage of 20 kV. Diamond quality and residual stress of the film were both investigated by Micro-Raman spectroscopy (Renishaw, inVia H 18415). The exciting source of the Raman system is a 514.5 nm argon ion laser with a power of 50 mW. A large-area mapping (around 5000 μm^2) with a point-focus mode (1 μm diameter) was used to achieve higher accuracy of the diamond peak shift and width which were identified using the curve-fitting option of the Raman software.

3. RESULTS AND DISCUSSION

3.1. Effects of the Different Pretreatments on the WC-Co Substrate. The surface morphology of the WC-Co substrate after each pretreatment was investigated by SEM and AFM (Figure 2). The as-received WC-Co substrates (Figures 2a and 2e) present a very smooth surface (Ra = 14 nm) with some grinding streaks caused by the production process. The P1 pretreatment, using the conventional chemical etching, changed the morphology of the substrate surface. The grains of WC were etched by the Murakami reagent and the cobalt-inserts were then removed by the acid attack, exposing the WC grain structure (Figure 2b). It can be seen that this pretreatment isotropically etches the surface. The corresponding AFM images (Figure 2f) shows that the surface roughness (Ra = 64 nm) increases compared to the untreated substrate (P0). After the laser irradiation (P2 pretreatment, Figures 2c and 2g), a periodic microroughness structure was created. The roughness significantly increased compared to the untreated substrate with a Ra value, measured by AFM, of around 94 nm. The last pretreatment (P3) presented the same periodic surface structure as P2. We can observe in the SEM micrograph (Figure 2d) a large number of small pits due to the preferential ablation of the cobalt inserts

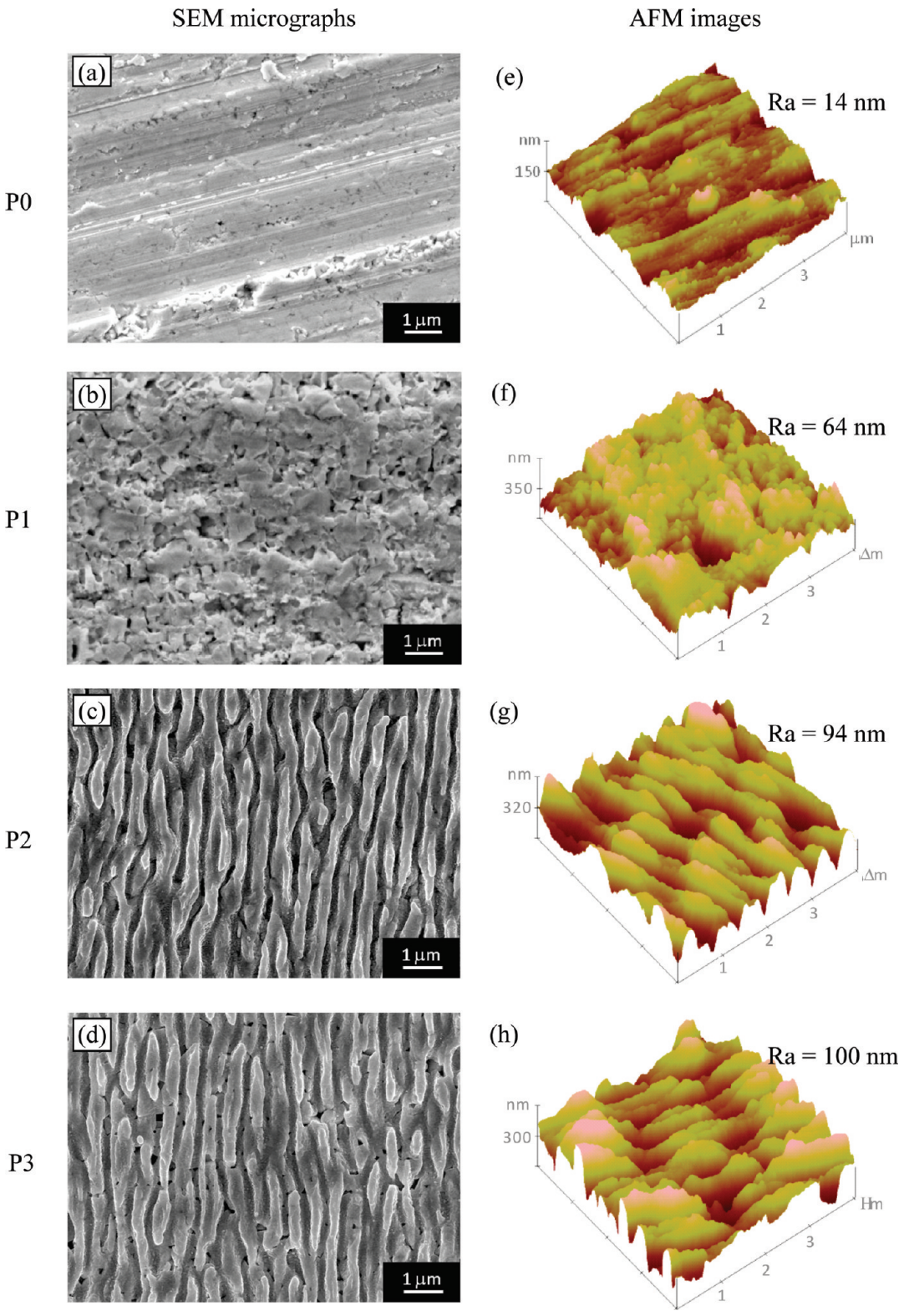

Figure 2. SEM micrographs and AFM images of WC-Co substrates with different pretreatments.

produced by the acid attack. The roughness of this substrate (Ra = 100 nm) is similar to that of P2.

The cobalt concentration on the substrate surface for each pretreatment was measured by EPMA. According to the EPMA resolution, the cobalt content was measured on a depth of 1 μm from the substrate surface. The results are given in table 2 and show that the cobalt concentration of the untreated substrate is about 4.5 wt %. The same concentration of cobalt was found after the P2 pretreatment. Therefore, the laser ablation leads to a modification of the surface roughness but has no influence on the cobalt content. To remove the cobalt, a chemical etching is needed, which is the role of the acid attack in the P1 and P3

pretreatments. Indeed the EPMA results show a decrease in the cobalt content after both pretreatments. The P1 pretreatment, a combination of a Murakami reagent and acid attack, is the most effective in removing the cobalt. In this pretreatment, the Murakami reagent is used for selectively attacking the WC and not the cobalt. Therefore after the etching with a Murakami reagent, the cobalt particles are left on the substrate surface and can be easily removed by the following acid attack. With the P3 pretreatment, however, the laser etches both WC and Co. It is more difficult to remove all cobalt with the acid attack. This explains the higher cobalt content with P3 than with P1.

Table 2. Variation of the Cobalt Concentration on Different WC-Co Substrates

pretreatment name	wt. % of cobalt
P0	4.5 ± 0.2
P1	0.4 ± 0.1
P2	4.7 ± 0.2
P3	1.1 ± 0.1

3.2. Microstructural Analyses of Diamond Films and Cobalt Content. Figure 3 shows the surface morphology of diamond films deposited on WC-Co substrates with the different pretreatments for two deposition times of 15 and 60 min. After 15 min of deposition, continuous diamond films were formed on the P0 and P1 substrates (Figure 3a and 3b respectively). For both films the diamond grains are about 2 μm in size and randomly oriented. In the two other pretreatments P2 and P3, (Figures 3c and 3d, respectively), diamond islands can be observed after 15 min of deposition and larger diamond grain size (close to 5 μm). After 60 min of deposition, a continuous diamond film with an average grain size ranging from 10 to 20 μm was formed on each substrate. The orientation of the diamond is completely random for the deposition on low-roughness substrates (P0 and P1, Figures 3e and 3f, respectively) while (100) crystal orientations are promoted by the laser treatment, as observed on substrates P2 (Figure 3g) and P3 (Figure 3h).

This difference on the diamond film morphology is linked to the growth process. Because of the very high surface energy of the diamond (>4 J m^{-2}), its growth is generally a 3-D process with

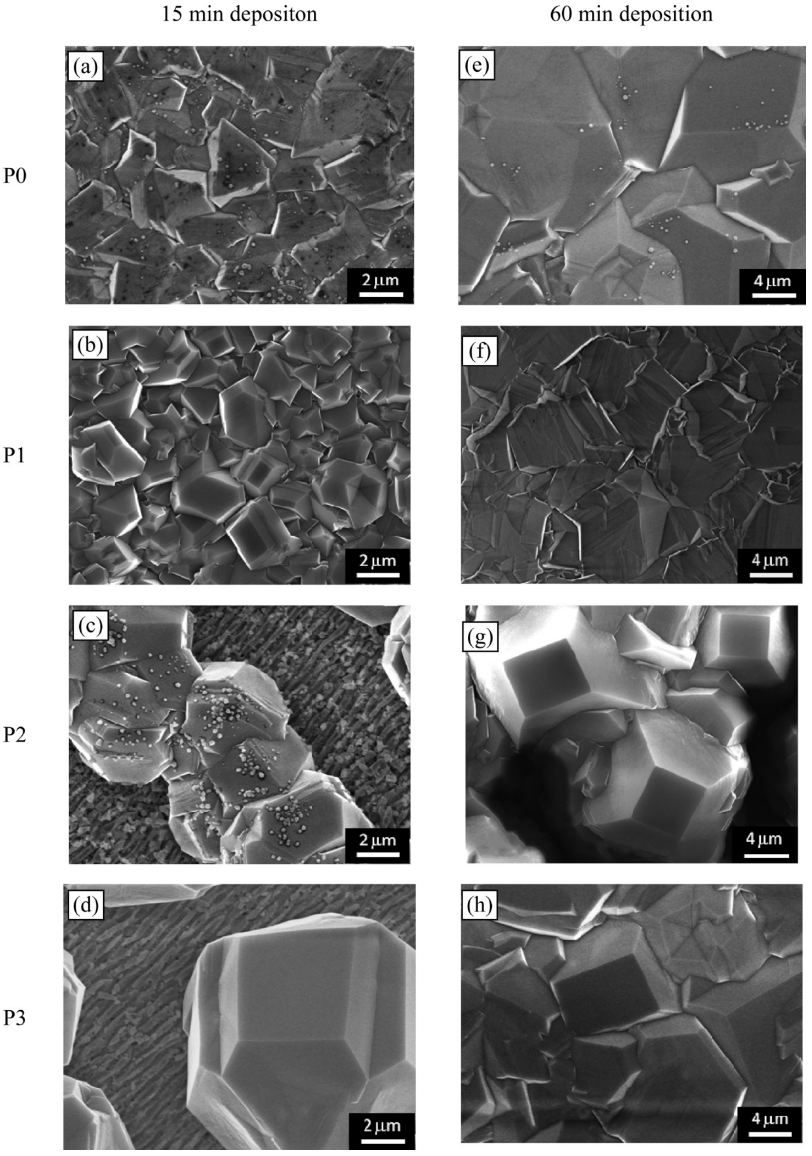

Figure 3. SEM micrographs of diamond films deposited for 15 and 60 min on WC-Co substrates with different pretreatments.

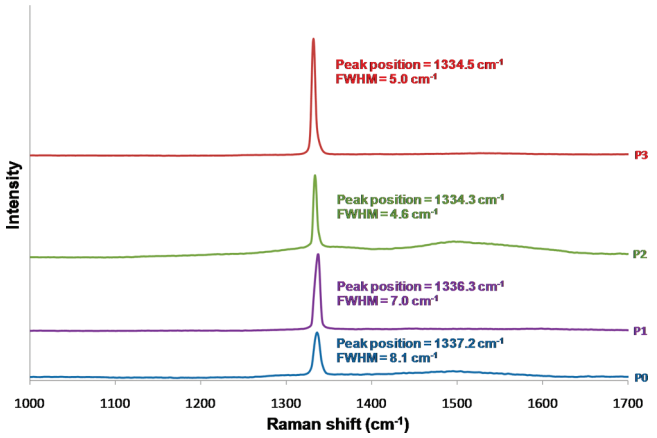

Figure 4. Raman spectra of diamond films deposited for 60 min on the different types of substrates.

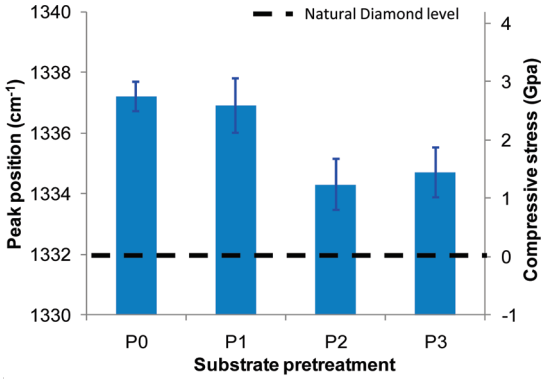

Figure 5. Raman peak shift and corresponding compressive stress in diamond films deposited on the different kinds of substrates.

island growth, called the Vollmer−Weber process. In the case of the P2 and P3 substrates, the periodic roughness created on the surface lead to a growth of the diamond nuclei preferentially inside the cavity of the material. This surface roughness enhances the growth of the diamond and a Stranski−Krastanov growth can be involved. This is characterized by both 2-D layers and 3-D islands growths. This type of process can explain the difference of crystal orientation observed in the laser-roughness substrate surfaces. Indeed, the roughness leads to a higher nucleation density which can allow the formation of 2-D diamond layers with a preferential orientation (100). After the creation of these 2-D layers, the growth process continues through a second nucleation on the oriented diamond layer with a 3-D process (island growth) and the formation of a continuous layer after coalescence.

In the SEM micrographs, presence of cobalt particles on the surfaces of the diamond grains are observed, for P0 and P2 (Figure 3a and 3c, respectively). During the deposition, performed at a high temperature (780 °C), the cobalt from the substrate bulk diffused continuously to the surface.[11] The presence of a large quantity of cobalt particles at the surface of the P2 substrate can be observed after deposition (Figure 3c) compared to the surface of P3 (Figure 3d), which has received the same irradiation treatment. However, the chemical etchings performed on samples P1 and P3 have removed the surface cobalt. Therefore, even though cobalt is still present in the bulk, it is sufficiently far from the surface (>1 μm) to prevent its migration into the diamond grains (Figure 3b and 3d) and to avoid its negative impact (nondiamond formation) on the diamond deposition.

3.3. Raman Spectroscopy of Diamond Films. Figure 4 shows the representative Raman spectra obtained from the diamond films deposited for 60 min on the different types of WC-Co substrates. All films show a sharp peak near 1332 cm^{-1}, which is characteristic of diamond. The average full widths at half-maximum (FWHM) of those peaks range from 4.6 to 8.1 cm^{-1} as compared with that of natural diamond (2.8−3.1 cm^{-1}).

We have also observed broad bands around 1375 and 1500 cm^{-1}, especially for P0 and P2. These bands are representative of nondiamond carbon content, with the former corresponding to the D-band of graphite and the latter to amorphous carbon.[20,21] For P0 and P2, the presence of these bands is in agreement with the large quantity of cobalt measured by EPMA. As explained previously, cobalt dissolves carbon and enhances the formation of graphitic and amorphous carbon phases.[12,13,22]

A systematic shift in the diamond Raman peak compared to pure diamond (1332 cm^{-1}) is detected, which corresponds to the residual stresses (σ) in the diamond films. The residual stress is proportional to the Raman peak shift and can be calculated in an unsplitted diamond peak as follows:[23−25]

$$\sigma = -0.567(\nu_m - \nu_0)$$

where ν_m and ν_0 are the Raman peak positions of stressed (measured) and unstressed (1332 cm^{-1}, natural diamond) diamond respectively.

Figure 5 shows the diamond peak position and the corresponding compressive stress, for each pretreatment. These values are average values from the Raman mapping analyses. All of the diamond films have compressive stresses. Because of the higher coefficient of thermal expansion of the WC-Co substrates (4.4×10^{-6} K^{-1}) compared to that of the diamond films (1.0×10^{-6} K^{-1}), the dilatation of the substrate during the deposition is greater than the diamond and therefore induces a compression of the diamond films after cooling.[25,26]

The diamond films deposited on P0 and P1 have higher compressive stresses than those on P2 and P3. These results confirm that the roughness induced by the laser treatment releases the stress in the films. This stress release can also be explained by the fact that fs laser processing is a thermal process unlike the chemical process. This reduction of the compressive stress is found to provide better film adhesion.[8] Therefore, if we simply consider the stress, the P2 and P3 treatments seem equivalent and are both beneficial for diamond deposition.

The quality of diamond films can be evaluated by the calculation of a quality factor (Q) with the following relationship:[27,28]

$$Q_{[514nm]} = \frac{I_{Diamond}}{\left(I_{Diamond} + \frac{I_{a\text{-}carbon}}{233}\right)} \times 100$$

where $I_{Diamond}$ and $I_{a\text{-}carbon}$ are the intensity of the diamond peak and the total intensity of the nondiamond carbon, respectively. The coefficient 233 corresponds to the Raman intensity ratio between amorphous carbon and diamond at an excitation wavelength of 514 nm. The quality factor plotted in Figure 6 is an average value calculated with a minimum of ten Raman spectra for each substrate pretreatment. This factor is higher than 99.9% for all pretreatments, confirming the high quality of the diamond prepared by the laser-assisted method. The diamond films deposited on P1 and P3 exhibit an extremely high quality factor

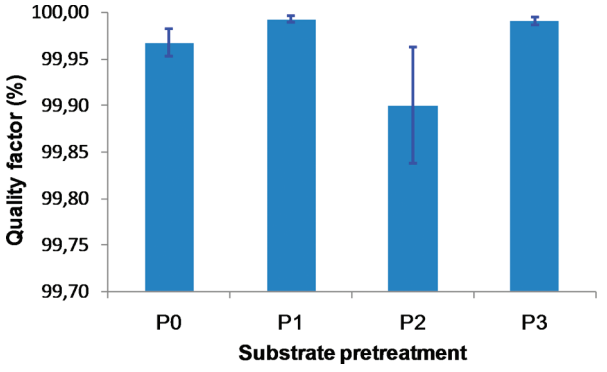

Figure 6. Quality factor of the diamond films deposited on the different kinds of substrates.

around 99.99%, corroborating the fact that little nondiamond carbon is found in these films. Furthermore this supports the idea that less cobalt content leads to less nondiamond carbon.

The quality factor, along with the other analyses performed in this paper, prove that the P3 pretreatment is the most promising for diamond deposition. This combination of laser irradiation and acid etching releases the stress in the film by increasing the roughness and at the same time eliminating the nondiamond carbon formation by removing the surface cobalt.

4. CONCLUSIONS

The effects of different WC-Co substrate pretreatments on the quality, cobalt content, and residual stresses of diamond films, deposited with a laser-assisted combustion flame method, have been investigated. It was found that the deposition method leads to the growth of high-quality polycrystalline diamond films. The chemical etching method (P1) was used to remove cobalt on the substrate surface, but the roughness introduced by this pretreatment hardly decreased the stresses in the film. On the other hand, laser etching (P2) did reduce the stresses, but the cobalt concentration remained high and produced a large quantity of nondiamond carbon. Finally, a combination of the two etchings (P3) provided as expected the advantages of a homogeneous high-quality and cobalt-free diamond film with low residual stress and thus high adhesion with the substrate.

AUTHOR INFORMATION

Corresponding Author

*Tel: 1-402-472-8323. E-mail: ylu2@unl.edu.

ACKNOWLEDGMENT

The authors would like to thank Dr. Y. Zhou form the Department of Vet & Biomedical Sciences at the University of Nebraska-Lincoln for providing convenient access to the SEM and Dr. L. Yue for her help to acquire the AFM images. This work was financially supported by the U.S. Office of Naval Research (ONR) through the Multidisciplinary University Research Initiative (MURI N00014-05-1-0432) program and grant N00014-09-1-0943.

REFERENCES

(1) Bundy, F. P.; Hall, H. T.; Strong, H. M.; Wentorf, R. H. *Nature* **1955**, *176*, 51–54.
(2) McCauley, T. S.; Vohra, Y. K. *Appl. Phys. Lett.* **1995**, *66*, 1486–1488.
(3) Hirose, H.; Komaki, K. Eur. Patent EP 324538, 1988.
(4) Ravi, K. V. *Diamond Relat. Mater.* **1995**, *4* (4), 243–249.
(5) Ling, H.; Sun, J.; Han, Y. X.; Gebre, T.; Xie, Z. Q.; Zhao, M.; Lu, Y. F. *J. Appl. Phys.* **2009**, *105* (1), 014901–014901-5.
(6) Xie, Z. Q.; Zhou, Y. S.; He, X. N.; Gao, Y.; Park, J. B.; Ling, H.; Jiang, L.; Lu, Y. F. *Cryst. Growth Des.* **2010**, *10* (4), 1762–1766.
(7) McKindra, T.; O'Keefe, M. J.; Xie, Z. Q.; Lu, Y. F. *Mater. Charact.* **2010**, *61* (6), 661–667.
(8) Lee, D. G.; Gilbert, D. R.; Lee, S. M.; Singh, R. K. *Compos. Part B* **1999**, *30* (7), 667–674.
(9) Cappelli, E.; Orlando, S.; Pinzari, F.; Napoli, A.; Kaciulis, S. *Appl. Surf. Sci.* **1999**, *138−139*, 376–382.
(10) Deuerler, F.; van den Berg, H.; Tabersky, R.; Freundlieb, A.; Pies, M.; Buck, V. *Diamond Relat. Mater.* **1996**, *5* (12), 1478–1489.
(11) Mallika, K.; Komanduri, R. *Wear* **1999**, *224* (2), 245–266.
(12) Donnet, J. B.; Paulmier, D.; Oulanti, H.; Le Huu, T. *Carbon* **2004**, *42* (11), 2215–2221.
(13) Peters, M. G.; Cummings, R. H. U.S. Patent 5236740, 1993.
(14) Cabral, G.; Madaleno, J. C.; Titus, E.; Ali, N.; Grácio, J. *Thin Solid Films* **2006**, *515*, 158–163.
(15) Polini, R.; Barletta, M. *Diamond Relat. Mater.* **2008**, *17* (3), 325–335.
(16) Wei, Q. P.; Yu, Z. M.; Ashfold, M. N. R.; Ye, J.; Ma, L. *Appl. Surf. Sci.* **2010**, *256* (13), 4357–4364.
(17) Han, Y. X.; Ling, H.; Lu, Y. F. *J. Appl. Phys.* **2006**, 100.
(18) Harzic, R.; Le; Huot, N.; Audouard, E.; Jonin, C.; Laporte, P.; Valette, S.; Fraczkiewicz, A.; Fortunier, R. *Appl. Phys. Lett.* **2002**, *80*, 3886.
(19) Ling, H.; Xie, Z. Q.; Gao, Y.; Gebre, T.; Shen, X. K.; Lu, Y. F. *J. Appl. Phys.* **2009**, *105*, 064901.
(20) Knight, D. S.; White, W. B. *J. Mater. Res.* **1989**, *4* (2), 385–393.
(21) Kromka, A.; Breza, J.; Kadleciková, M.; Janik, J.; Balon, F. *Carbon* **2005**, *43* (2), 425–429.
(22) Xu, Z.; Lev, L.; Lukitsch, M.; Kumar, A. *Diamond Relat. Mater.* **2007**, *16* (3), 461–466.
(23) Ager, J. W.; Drory, M. D. *Phys. Rev. B* **1993**, *48*, 2601–2607.
(24) Kim, J. S.; Cappelli, M. A. *J. Appl. Phys.* **1992**, *72* (11), 5461–5466.
(25) Hua Fan, Q.; Grácio, J.; Pereira, E. *Diamond Relat. Mater.* **2000**, *9*, 1739–1743.
(26) Ralchenko, V. G.; Smolin, A. A.; Pereverzev, V. G.; Obraztsova, E. D.; Korotoushenko, K. G.; Konov, V. I.; Lakhotkin, Y. V.; Loubnin, E. N. *Diamond Relat. Mater.* **1995**, *4* (5−6), 754–758.
(27) Sails, S. R.; Gardiner, D. J.; Bowden, M.; Savage, J.; Rodway, D. *Diamond Relat. Mater.* **1996**, *5* (6−8), 589–591.
(28) Bak, G. W.; Fabisiak, K.; Klimek, L.; Kozanecki, M.; Staryga, E. *Opt. Mater.* **2008**, *30* (5), 770–773.